

Large Language Models Powered Context-aware Motion Prediction

Xiaoji Zheng, Lixiu Wu, Zhijie Yan, Yuanrong Tang, Hao Zhao
Chen Zhong[✉], Bokui Chen[✉], and Jiangtao Gong[✉]

Abstract—Motion prediction is among the most fundamental tasks in autonomous driving. Traditional methods of motion forecasting primarily encode vector information of maps and historical trajectory data of traffic participants, lacking a comprehensive understanding of overall traffic semantics, which in turn affects the performance of prediction tasks. In this paper, we utilized Large Language Models (LLMs) to enhance the global traffic context understanding for motion prediction tasks. We first conducted systematic prompt engineering, visualizing complex traffic environments and historical trajectory information of traffic participants into image prompts—Transportation Context Map (TC-Map), accompanied by corresponding text prompts. Through this approach, we obtained rich traffic context information from the LLM. By integrating this information into the motion prediction model, we demonstrate that such context can enhance the accuracy of motion predictions. Furthermore, considering the cost associated with LLMs, we propose a cost-effective deployment strategy: enhancing the accuracy of motion prediction tasks at scale with 0.7% LLM-augmented datasets. Our research offers valuable insights into enhancing the understanding of traffic scenes of LLMs and the motion prediction performance of autonomous driving.

I. INTRODUCTION

Motion prediction is one of the most important tasks in the field of autonomous driving [1]–[3], which predicts the motion statuses of nearby agents by jointly considering nearby agents and road maps. This information will assist the decision module in making a more robust and safer driving decision. Therefore, this field already features a plethora of datasets and public competitions. For instance, since 2021, Waymo has been organizing competitions in motion prediction¹, attracting models and algorithms that have won championships, such as MTR [1], MTR++ [2], and MGTR [4]. There are three classes of motion prediction methods: goal-based methods [5], [6], direct-regression methods [7], [8], and methods that take the best of both [1], [2]. Although methods that take the best of both can balance results and computing resources greatly, they still encode information about agents and maps first and then decode to obtain final results. The methods above all lack a comprehensive understanding of overall traffic semantics.

Large Language Model (LLM) is popular in the field of autonomous driving, as not only the Language Model but also the World Model with common sense [9]–[11].

The authors are with the Institute for AI Industry Research, Tsinghua University, Beijing, China. Corresponding Email: myheimu@gmail.com, chenbk@tsinghua.edu.cn, gongjiangtao@air.tsinghua.edu.cn

¹<https://waymo.com/open/challenges/2021/motion-prediction/>

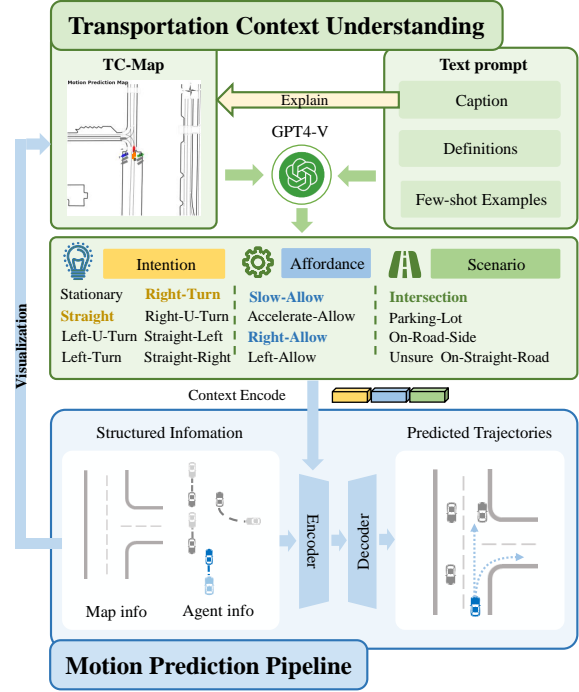


Fig. 1. Context-aware Motion Prediction Based on LLMs. We first visualize structured information in the motion prediction dataset, GPT4-V then understand the scenario we provided via visualized image and well-designed prompt and output transportation context information. This information will be used to augment traditional motion prediction algorithms.

After the release of OpenAI’s GPT series of large language models, many works that use GPT to assist driving have been emerging [12]–[16]. These efforts leverage the inferential capabilities of large language models or through experimentation, aiding autonomous driving algorithms in better perception [17] and planning [12], [14], [15], and even facilitating end-to-end decision-making [13], [18]. However, teaching LLM to understand the interactive context among various transportation participants in diverse transportation scenarios is still a challenging task. Although many have applied vision-language models to traffic scenarios, their performance heavily relies on datasets annotated from a first-person perspective [19]–[21]. For abstract, information-overwhelming, and bird’s-eye view traffic scenarios, there is a lack of relevant datasets and understanding methodologies.

In this paper, we propose a new method that enhances the traffic context understanding of motion prediction models using LLMs to make more accurate predictions. To enable an unfine-tuned LLM—GPT4 with vision (GPT4-

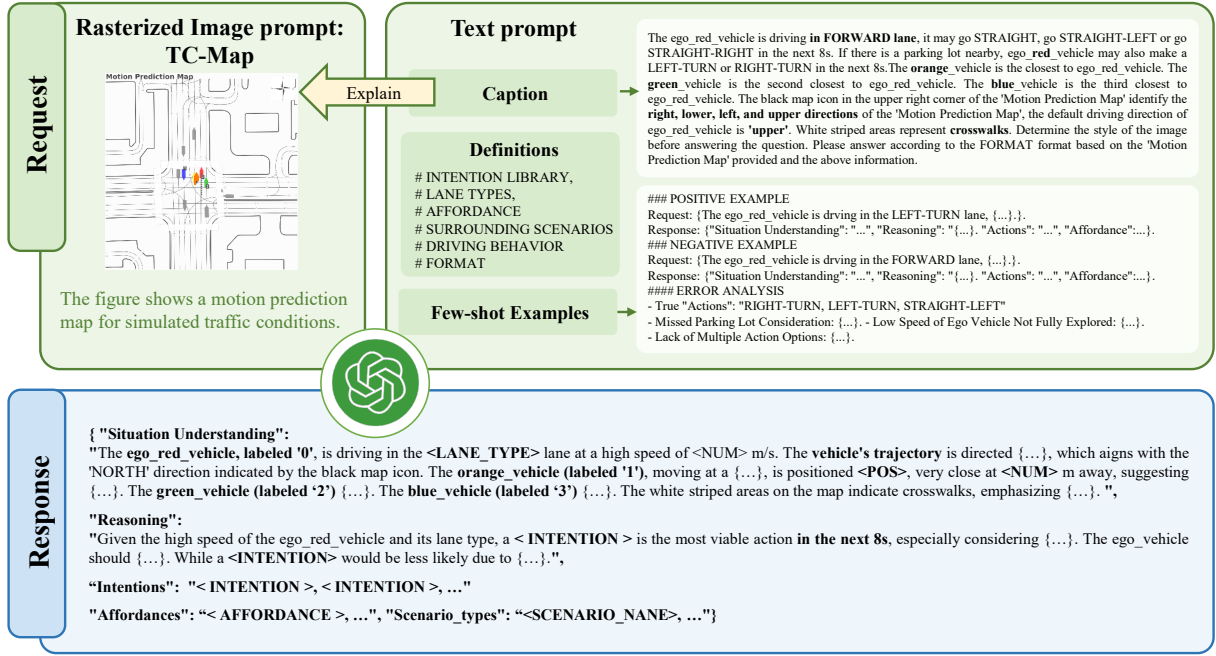


Fig. 2. Details of Transportation Context Generation Prompt.

V) to understand traffic context and output the necessary context information for motion prediction, we visualize the vector map data and historical data of traffic participants as a Transportation Context Map (TC-Map) to serve as an image prompt and propose a corresponding text prompt design. After successfully obtaining traffic context information generated by the LLM, we integrated this information into a classical motion prediction algorithm—MTR [1]. The results indicate that this context information effectively improves the accuracy of motion prediction. Additionally, considering the cost of LLMs, we also propose a cost-effective deployment strategy: by utilizing 0.7% LLM-enhanced datasets, we can empower motion prediction performance at scale.

Our contributions are as follows:

- We systematically designed and conducted prompt engineering to enable an unfine-tuned GPT4-V to comprehend complex traffic scenarios involving multiple participants and to output context information such as intention, affordance, and scenario;
- We introduced a novel approach that combines the context information outputted by GPT4-V with the classical motion prediction pipeline [1], and we verified that this method enhances the effectiveness of motion prediction;
- We proposed and validated a deployment strategy based on a dataset with a limited amount of LLM-generative context, which reduced the deployment cost of this method.

II. METHOD

A. Get Transportation Context from GPT4-V

Translating images directly into motion poses is significantly challenging [22]. We obtain transportation context

through methods based on LLMs with vision, defining the interested agent in the TC-Map as the ego-agent, which includes three categories: vehicle, pedestrian and cyclist. As shown in Fig. 2, the TC-Map designed based on the WOMD serves as the Rasterized Image prompt, and together with the Text prompt forms the Transportation Context Generation Prompt (TCGP). Through GPT4-V, this input yields outputs such as Situation Understanding, Reasoning, Intentions of ego-agent, Affordances [23], and Scenario Types. Additionally, during the prompt design process, we summarized 6 prompt design suggestions as shown in Fig. 3.

1) *TC-Map design suggestions:* Corresponding to Prompt Design Suggestion 1 and 2 in Fig. 3. Suggestion 1 aims to reduce confusion in the volume of information. Inspired by the MTR Map Collection module, we introduced TC-Map Crop. Additionally, during the initial testing of GPT4-V, it was found that embedding a large amount of data information in the Text prompt, such as 11 frames of historical trajectory in JSON format, easily confuses GPT4-V and increases the uncertainty of intent. So the extent of TC-Map is cropped based on the type of agent (vehicle: pedestrian: cyclist = 6:4:3), limiting the ego-agent to focus only on the appropriate surrounding area scenes, reducing the impact of irrelevant factors on the prediction of Intention. Suggestion 2 aims to minimize confusion in direction identification. The diversity of scenarios leads to a variety of headings for the ego-agent, a common map guide icon is selected to normalize the heading of the ego-agent to "North".

2) *Text Prompt design suggestions:* Corresponding to Prompt Design Suggestion 3 and 4 in Fig. 3. Suggestion 3 proposes Examples, divided into Positive and Negative categories. Positive Examples adhere to the randomness and diversity of intent generation. Negative Examples are bad

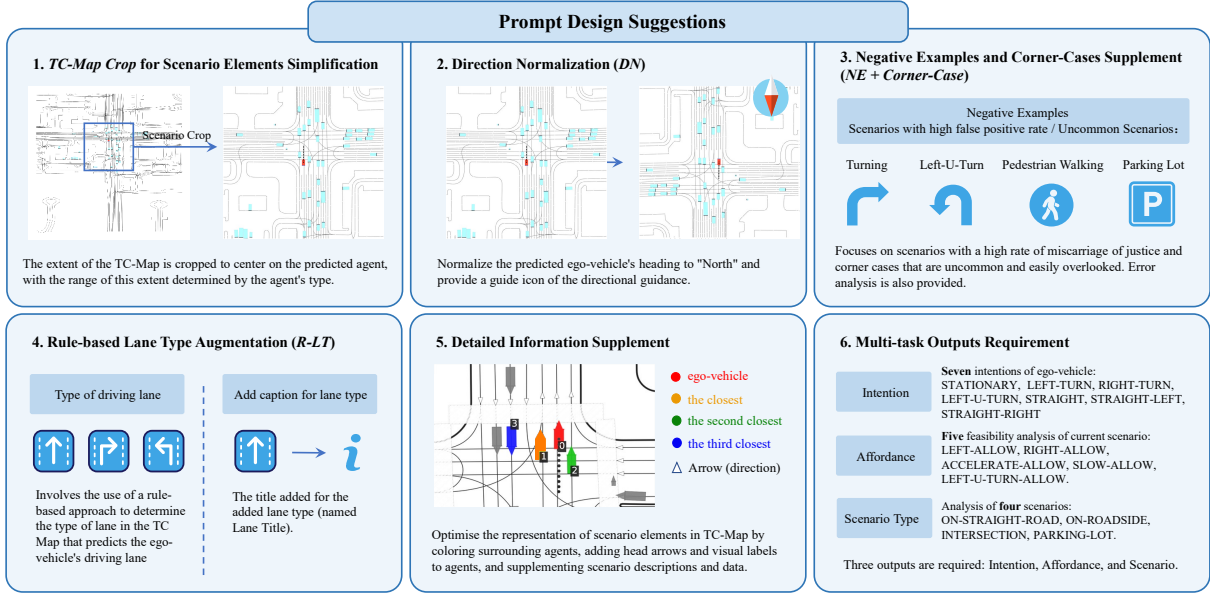


Fig. 3. Six Prompt Design Guideline for GPT4-V Understanding Motion Predication Context.

cases selected from GPT4-V's responses during the quantitative experiment of prompts, focusing on scenarios with high misjudgment rates and uncommon, easily overlooked Corner-Cases. Additional Error Analysis is provided and placed closer to the end of the Text prompt. Suggestion 4 consists of two sentences. The first sentence discusses using rules to determine the lane type of the ego-agent's driving lane in TC-Map, the second sentence provides explanations for the added lane types, they assist GPT4-V in excluding impossible intents under the premise that the ego-agent follows traffic rules, based on traffic driving regulations.

3) *Detailed Information Supplement*: Corresponding to Prompt Design Suggestion 5 in Fig. 3. To fully leverage the scene information from WOMP dataset, such as road edges and crosswalks, we optimize the representation of different types of scenario information in TC-Map by adding more indicative head arrows and visual labels for agents. During this phase, we also incorporate the speed of the ego-agent, as well as the speed, relative positions, and distances of the surrounding three agents.

4) *Multi-task Outputs Requirement*: Corresponding to Prompt Design Suggestion 6 in Fig. 3, we designed seven types of Intentions for the ego-agent over the next 8 seconds. *STRAIGHT-LEFT* and *STRAIGHT-RIGHT* are considered scenarios where future ego-agent merging might occur, indicating complex intentions. Predicting these intentions often requires GPT4-V to utilize rasterized images, the ego-agent's own position, heading, and speed, the state of surrounding vehicles, and the direction of nearby lane lines predicting these two types of intentions highly challenging. Additionally, based on an understanding of complex scenes, we designed five types of Affordances and four types of Scenario types, collectively providing a rich, human-like transportation context information to enhance the accuracy of the motion prediction task.

B. Augment Motion Prediction Models via Transportation Context information

1) *Motion Transformer*: We choose Motion TTransformer (MTR), SOTA of WOMB Challenge 2022, as our base model. MTR is developed based on the architecture of Transformer [24]. It first encodes the scenario information including agents and map roads, and then obtains the motion trajectories after several decoding processes.

2) *Integrate with Transportation Context Information*: The transportation context contains three types of information: **intention**, **affordance** [23], and **scenario** in the format of a list, in which each element is a natural language description word. For example, ["STRAIGHT", "RIGHT-TURN"], ["SLOW-ALLOW", "RIGHT-ALLOW"], and ["INTERSECTION"] in Fig. 1, respectively. As the number of each type of context information is fixed, we use one-hot vectors to express the context information. In addition, because the description words in the list are not exclusive, we allow several '1's to appear in the one-hot vector.

More specifically, for affordance and scenario information generated by LLM, we simply encode the nature language into one-hot vectors:

$$A = \text{OneHotEncode}(\text{AffordanceList}), \quad (1)$$

$$S = \text{OneHotEncode}(\text{ScenarioList}), \quad (2)$$

where $A \in \mathbb{R}^8$ and $S \in \mathbb{R}^4$ (see Fig. 1). As the number of ground truth intentions is only one, the number of description words in the intention information list is not strictly one. LLM gives possible intentions and the order of different words stands for different possibilities. So, when we encode intention information into a one-hot vector, we set different weights for different intentions in the list:

$$I = \text{WeightedOneHotEncode}(\text{IntentionList}). \quad (3)$$

TABLE I
EFFECTS OF DIFFERENT COMPONENTS IN TRANSPORTATION CONTEXT GENERATION PROMPT.

<i>Sugg 1</i>	<i>Sugg 2</i>	<i>Sugg 3</i>	<i>Sugg 4</i>	<i>Sugg 5</i>		<i>ACC(Ist-I)</i>	<i>ACC</i>	<i>ACC(S,S-L,S-R)</i>
TC-Map Crop	DN	NE+Corner-Case	R-LT	TCGP-Opt	SPD-Add			
✗	✗	✗	✗	✗	✗	0.3551	0.5140	0.5794
✓	✗	✗	✗	✗	✗	0.4579	0.5981	0.7383
✓	✓	✗	✗	✗	✗	0.4205	0.6635	0.7757
✓	✓	✓	✗	✗	✗	0.4112	0.6822	0.8037
✓	✓	✓	✓	✗	✗	0.5607	0.8317	0.9252
✓	✓	✓	✓	✓	✗	0.5514	0.8691	0.9252
✓	✓	✓	✓	✓	✓	0.5794	0.8691	0.9345

Sugg: Prompt Design Suggestions. **TCGP-Opt**: Coloring the agents surrounding the red ego-agent in different colors to distinguish them easily and optimizing the representation of scene elements in the TC-Map and supplementing the corresponding scene description in text prompts. **SPD-Add**: Adding information about the speed of the ego-agent, the speeds of surrounding agents, and their relative positions and distances to the ego-agent in text prompts. **ACC**: The accuracy of intentions output by GPT4-V. When GPT4-V outputs multiple intentions, if at least one intention matches the ground truth without additional clarification, it is considered correct. *Ist-I*: Taking only the first intention from the list of intentions output by GPT4-V. (*S,S-L,S-R*) means consolidating the three intentions of *STRAIGHT*, *STRAIGHT-LEFT*, and *STRAIGHT-RIGHT* into a single *STRAIGHT* category.

The weight for i -th word in the list is:

$$weight_i = length(IntentionInfoList) - i, \quad (4)$$

where $I \in \mathbb{R}^5$ (see Fig. 1). So that the first word in the list has the maximal weight, and the last word holds the minimal weight.

To improve the performance of motion prediction and reduce the cost of computing resources, cluster-based intention points were provided in the process of decoding as prior knowledge [1]. Inspired by this, we also choose to integrate the transportation context information generated by LLM in the process of decoding.

The query content $Q \in \mathbb{R}^{K \times D}$ includes all scenario information in the data, where K stands for the number of trajectories that need to be predicted and D is the dimension of the feature. We first concatenate different types of context information and align the dimensions of traffic context information with query content, then integrate the context information generated by LLM via cross-attention after query content has been initialized.

$$TC = MLP([I, A, S]), \quad (5)$$

$$TC = RepeatFirstDim(TC, K), \quad (6)$$

$$Q_{tc} = CrossAttn(q = Q_0, k = TC, v = TC), \quad (7)$$

where $TC \in \mathbb{R}^D$ in Eq. 5 after multi-layer perceptron, and $TC \in \mathbb{R}^{K \times D}$ after repeating K times in Eq. 6. When conducting cross-attention, we use initialized query content Q_0 as query, and TC for both key and value in Eq. 7.

The following pipeline keeps all the same with MTR.

III. EXPERIMENT

A. Data distribution

We created a confusion matrix for the results in Tab. II as shown in Fig. 4, where we have merged *STRAIGHT-LEFT* and *STRAIGHT-RIGHT* into *STRAIGHT*. In this matrix, the rows represent the Ground Truth intentions, while the columns represent the intentions predicted by GPT4-V. Observing the main diagonal of the confusion matrix, it's

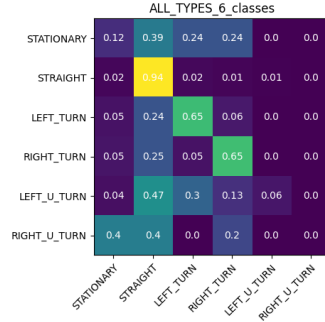


Fig. 4. Confusion Matrix of Intention Generated from GPT4-V

TABLE II
DATA AND INTENTION ACCURACY OF THREE EGO-AGENT TYPES.

method	type	<i>ACC(Ist-I)</i>	<i>ACC</i>	<i>ACC(S,S-L,S-R)</i>
MTR	V	0.8097	0.9442	0.9635
	P	0.6906	0.9495	0.9564
	C	0.7226	0.8822	0.9321
	AVG	0.76448	0.93211	0.95326
GPT4-V	V	0.6224	0.8482	0.9080
	P	0.6222	0.8038	0.8133
	C	0.5838	0.7857	0.9030
	AVG	0.6145	0.8259	0.8865

not hard to see that *STRAIGHT* has the highest prediction accuracy, followed by *LEFT_TURN* and *RIGHT_TURN* predictions. The lower prediction accuracy for *STATIONARY* is primarily because it can be correctly identified only when the ego-agent's speed is zero. Nevertheless, its Ground Truth is classified as *STATIONARY* even at very low speeds. Ego-agents intended for *LEFT_U_TURN* are frequently classified as *LEFT_TURN*, a consequence of the WOMD map's left-turn lanes occasionally accommodating straight movements, thus increasing the likelihood of *LEFT_U_TURN* and *LEFT_TURN* being predicted as *STRAIGHT*. Similarly, *RIGHT_U_TURN* ego-agents are often mistaken as

STRAIGHT, and unexpectedly, they are frequently classified as *STATIONARY*. This anomaly primarily arises because intentions like *RIGHT_U_TURN* are most common among pedestrians, whose speed and walking direction can change abruptly, posing significant challenges to accurately predicting their intentions. We also present the results of MTR, even though the result of GPT-4V on Intention is lower than MTR, it can also provide information for motion prediction and improve the accuracy of MP as shown in Tab. III.

B. Ablation Study of TCGP

We perform ablation studies on TCGP to understand the effectiveness of each component. As shown in Tab. I,

The data for the ablation experiment were randomly sourced from the WOMB testing set, comprising 107 TC-Maps samples. We have the following observations: **1)** TCGP achieves optimal performance when fully equipped with all its components, with every module playing a role in predicting intentions. **2)** TC-Map Crop enables GPT4-V to allocate more attention to the areas that should be focused on when predicting the future intentions of the ego-agent, significantly enhancing the accuracy of intention prediction. **3)** R-LT is crucial because it provides the type of lane in which the ego-agent is located, and the type of lane often determines the future direction of the vehicle.

C. LLM Augmented Motion Prediction

Dataset and metrics. We evaluate our methods and MTR on the large-scale WOMB [25]. For the task on WOMB, 1 second of history data will be provided, and 6 motion trajectories of the agents for 8 seconds in the future are needed. We utilize the official evaluation tool to calculate the evaluation metric, in which the mAP and miss rate (MR) are the most important ones in the official leaderboard ².

Data generation. There are roughly 2 million agents in WOMB and our prompt (text prompt and image prompt) costs about \$0.1 for each agent. So generating the transportation context information for all agents in WOMB costs nearly \$200,000. As it is costly to use GPT4-V for each agent in WOMB, we first generate the transportation context information from a minimal part of WOMB and then generate similar transportation context information for the remaining part via the nearest neighbor algorithm (see Alg.1). We first split the overall dataset into two different parts: T_1 and T_2 , LLM will generate transportation context information for T_2 . Secondly, we encode the scenario information for each agent in T_1 and T_2 and obtain their feature vectors. Finally, for each agent A_i in T_1 , the similar transportation context is the same as the agent A_j in T_2 that has the closest distance with A_i . More specifically, we use Euclidean distance in the nearest neighbor finding algorithm.

Performance comparison. We compared our LLM augmented motion prediction model with MTR on the validation set of WOMB. We trained both models on 20% WOMB

Algorithm 1 Generate Scaled LLM Augmented Training Data with Minimal LLM Augmented Data

Input: T : the overall dataset without LLM augmented;
Encoder: scenario info encoder; *LLM*: large language model.

Output: T^* : the overall dataset with LLM augmented.

- 1: initial $T_1, T_2 \leftarrow \text{split}(T)$, where $|T_1| \gg |T_2|$
- 2: $TC_1 \leftarrow []$, where TC_1 is Transportation Context info
- 3: $TC_2 \leftarrow \text{LLM}(T_2)$
- 4: $F_1 \leftarrow \text{Encoder}(T_1)$, where F_1 is feature vector list
- 5: $F_2 \leftarrow \text{Encoder}(T_2)$
- 6: **for** agent i in T_1 **do**
- 7: $f_i \leftarrow F_1[i]$, where f_i is a feature vector
- 8: $j \leftarrow \text{NearestNeighbor}(f_i, F_2)$
- 9: $TC_1[i] = TC_2[j]$
- 10: **end for**
- 11: $T_1^* \leftarrow \text{Concatenate}(T_1, TC_1)$
- 12: $T_2^* \leftarrow \text{Concatenate}(T_2, TC_2)$
- 13: $T^* \leftarrow \text{Concatenate}(T_1^*, T_2^*)$

TABLE III
PERFORMANCE ON THE VALIDATION SET OF WOMB

method	type	mAP \uparrow	minADE \downarrow	minFDE \downarrow	MR \downarrow
MTR	V	0.3862	0.8257	1.6789	0.1809
	P	0.3587	0.3825	0.8088	0.0935
	C	0.2848	0.7985	1.6380	0.2212
	AVG	0.3432	0.6689	1.3752	0.1652
+LLM	V	0.3954	0.8147	1.6205	0.1751
	P	0.3754	0.3830	0.8070	0.0934
	C	0.2924	0.8102	1.6464	0.2306
	AVG	0.3527	0.6693	1.3580	0.1664

Performance Comparison. With LLM-augmented traffic context information, the motion prediction accuracy of different traffic agents improved. The best scores are expressed in **bold**.

dataset. Our main results are in Table III. V, P, C are abbreviations of vehicle, pedestrian, cyclist, respectively. The result shows that our LLM augmented motion prediction model (with generated similar context information) outperformed MTR among all three agents (i.e. vehicle, pedestrian, and cyclist), and the average mAP increased by 0.95% compared with MTR.

Ablation Study. This study evaluates the contribution of each component within the transportation context generated by the LLM toward enhancing motion prediction accuracy. An ablation experiment was conducted by randomly selecting 5% of scenarios (approximately 24,000 scenarios) from the WOMB training set. The evaluation involved comparing the baseline model against the LLM-augmented model on the minimal part of WOMB validation set with traffic context information generated by LLM. The results are presented in Table IV. I, A, and S are abbreviations of intention, affordance, and scenario, respectively. V-mAP, P-mAP, and C-mAP mean mAP scores for vehicle, pedestrian, and cyclist, respectively. The results highlight the incremental value added by incorporating various types of transportation con-

²<https://waymo.com/open/challenges/2023/motion-prediction/>

TABLE IV
ABLATION EXPERIMENT OF
LLM AUGMENTED MOTION PREDICTION

method	I	A	S	mAP	V-mAP	P-mAP	C-mAP
MTR	-	-	-	0.2970	0.3300	0.3507	0.2102
-	✓	-	-	0.3066	0.3377	0.3400	0.2422
-	-	✓	-	0.2995	0.3386	0.3277	0.2322
-	-	-	✓	0.3059	0.3341	0.3564	0.2272
-	✓	✓	-	0.3030	0.3294	0.3458	0.2337
-	✓	-	✓	0.3134	0.3318	0.3692	0.2392
-	-	✓	✓	0.3117	0.3389	0.3554	0.2409
+LLM	✓	✓	✓	0.3137	0.3385	0.3549	0.2476

Ablation Experiment. Results demonstrate that the model that uses three types of transportation context information gets the highest mAP score. The highest mAP score for each types of agent and average mAP score are expressed in **bold**.

text information. Specifically, augmenting the model with all three types of transportation context information yielded the highest mAP score. Compared to the baseline MTR model, the final LLM-augmented model demonstrated a significant improvement, with a 1.67% increase in the mAP score.

IV. CONCLUSIONS

In this paper, through systematic prompt engineering, we utilized the common sense and reasoning abilities of LLMs to extract human-like global context information from complex traffic scene motion predictions. By integrating these contexts into the traditional motion prediction pipeline, we enhanced the accuracy of trajectory prediction. We also proposed a cost-effective deployment strategy and verified its effectiveness.

Through meticulous prompt design, we achieved an impressive accuracy rate, underscoring the remarkable capacity of LLMs to comprehend complex and detailed transportation scenarios. To our knowledge, our work is pioneering in incorporating BEV-like TC-Maps into LLM prompts, offering a novel perspective for LLMs to interpret driving scenarios. Our experimental findings suggest that integrating transportation context information significantly enhances motion prediction capabilities. It is noteworthy that enabling LLMs to understand complex scene information remains challenging. Significant opportunities exist for exploring the integration of rich contextual information with motion prediction models. Our preliminary results suggest considerable potential for future development in this research area.

REFERENCES

- [1] S. Shi, L. Jiang, D. Dai, and B. Schiele, "Motion transformer with global intention localization and local movement refinement," *Advances in Neural Information Processing Systems*, vol. 35, pp. 6531–6543, 2022.
- [2] S. Shi, L. Jiang, D. Dai, and S. Bernt, "Mtr++: Multi-agent motion prediction with symmetric scene modeling and guided intention querying," 2024.
- [3] T. Zhao, Y. Xu, M. Monfort, W. Choi, C. Baker, Y. Zhao, Y. Wang, and Y. N. Wu, "Multi-agent tensor fusion for contextual trajectory prediction," in *Proceedings of the IEEE/CVF conference on computer vision and pattern recognition*, 2019, pp. 12 126–12 134.
- [4] Y. Gan, H. Xiao, Y. Zhao, E. Zhang, Z. Huang, X. Ye, and L. Ge, "Mgtr: Multi-granular transformer for motion prediction with lidar," *arXiv preprint arXiv:2312.02409*, 2023.

- [5] J. Gu, C. Sun, and H. Zhao, "Densetnt: End-to-end trajectory prediction from dense goal sets," in *Proceedings of the IEEE/CVF International Conference on Computer Vision*, 2021, pp. 15 303–15 312.
- [6] H. Zhao, J. Gao, T. Lan, C. Sun, B. Sapp, B. Varadarajan, Y. Shen, Y. Shen, Y. Chai, C. Schmid, *et al.*, "Tnt: Target-driven trajectory prediction," in *Conference on Robot Learning*. PMLR, 2021, pp. 895–904.
- [7] J. Ngiam, B. Caine, V. Vasudevan, Z. Zhang, H.-T. L. Chiang, J. Ling, R. Roelofs, A. Bewley, C. Liu, A. Venugopal, *et al.*, "Scene transformer: A unified architecture for predicting multiple agent trajectories," *arXiv preprint arXiv:2106.08417*, 2021.
- [8] B. Varadarajan, A. Hefny, A. Srivastava, K. S. Refaat, N. Nayakanti, A. Corrmann, K. Chen, B. Douillard, C. P. Lam, D. Angelov, *et al.*, "Multipath++: Efficient information fusion and trajectory aggregation for behavior prediction," in *2022 International Conference on Robotics and Automation (ICRA)*. IEEE, 2022, pp. 7814–7821.
- [9] J. Wei, X. Wang, D. Schuurmans, M. Bosma, F. Xia, E. Chi, Q. V. Le, D. Zhou, *et al.*, "Chain-of-thought prompting elicits reasoning in large language models," *Advances in Neural Information Processing Systems*, vol. 35, pp. 24 824–24 837, 2022.
- [10] X. Wang, J. Wei, D. Schuurmans, Q. Le, E. Chi, S. Narang, A. Chowdhery, and D. Zhou, "Self-consistency improves chain of thought reasoning in language models," *arXiv preprint arXiv:2203.11171*, 2022.
- [11] S. Yao, D. Yu, J. Zhao, I. Shafran, T. L. Griffiths, Y. Cao, and K. Narasimhan, "Tree of thoughts: Deliberate problem solving with large language models," *arXiv preprint arXiv:2305.10601*, 2023.
- [12] J. Mao, Y. Qian, H. Zhao, and Y. Wang, "Gpt-driver: Learning to drive with gpt," *arXiv preprint arXiv:2310.01415*, 2023.
- [13] Z. Xu, Y. Zhang, E. Xie, Z. Zhao, Y. Guo, K. K. Wong, Z. Li, and H. Zhao, "Drivegpt4: Interpretable end-to-end autonomous driving via large language model," *arXiv preprint arXiv:2310.01412*, 2023.
- [14] W. Wang, J. Xie, C. Hu, H. Zou, J. Fan, W. Tong, Y. Wen, S. Wu, H. Deng, Z. Li, *et al.*, "Drivemlm: Aligning multi-modal large language models with behavioral planning states for autonomous driving," *arXiv preprint arXiv:2312.09245*, 2023.
- [15] J. Mao, J. Ye, Y. Qian, M. Pavone, and Y. Wang, "A language agent for autonomous driving," *arXiv preprint arXiv:2311.10813*, 2023.
- [16] Y. Jin, X. Shen, H. Peng, X. Liu, J. Qin, J. Li, J. Xie, P. Gao, G. Zhou, and J. Gong, "Surrealdriver: Designing generative driver agent simulation framework in urban contexts based on large language model," *arXiv preprint arXiv:2309.13193*, 2023.
- [17] C. Sima, K. Renz, K. Chitta, L. Chen, H. Zhang, C. Xie, P. Luo, A. Geiger, and H. Li, "Drivelm: Driving with graph visual question answering," *arXiv preprint arXiv:2312.14150*, 2023.
- [18] T.-H. Wang, A. Maalouf, W. Xiao, Y. Ban, A. Amini, G. Rosman, S. Karaman, and D. Rus, "Drive anywhere: Generalizable end-to-end autonomous driving with multi-modal foundation models," *arXiv preprint arXiv:2310.17642*, 2023.
- [19] D. Wu, W. Han, T. Wang, Y. Liu, X. Zhang, and J. Shen, "Language prompt for autonomous driving," *arXiv preprint arXiv:2309.04379*, 2023.
- [20] T. Qian, J. Chen, L. Zhuo, Y. Jiao, and Y.-G. Jiang, "Nuscenes-qa: A multi-modal visual question answering benchmark for autonomous driving scenario," *arXiv preprint arXiv:2305.14836*, 2023.
- [21] M. Nie, R. Peng, C. Wang, X. Cai, J. Han, H. Xu, and L. Zhang, "Reason2drive: Towards interpretable and chain-based reasoning for autonomous driving," *arXiv preprint arXiv:2312.03661*, 2023.
- [22] K. Chitta, A. Prakash, and A. Geiger, "Neat: Neural attention fields for end-to-end autonomous driving," in *Proceedings of the IEEE/CVF International Conference on Computer Vision*, 2021, pp. 15 793–15 803.
- [23] Y. Xu, X. Yang, L. Gong, H.-C. Lin, T.-Y. Wu, Y. Li, and N. Vasconcelos, "Explainable object-induced action decision for autonomous vehicles," in *Proceedings of the IEEE/CVF Conference on Computer Vision and Pattern Recognition*, 2020, pp. 9523–9532.
- [24] A. Vaswani, N. Shazeer, N. Parmar, J. Uszkoreit, L. Jones, A. N. Gomez, L. Kaiser, and I. Polosukhin, "Attention is all you need," *Advances in neural information processing systems*, vol. 30, 2017.
- [25] S. Ettinger, S. Cheng, B. Caine, C. Liu, H. Zhao, S. Pradhan, Y. Chai, B. Sapp, C. R. Qi, Y. Zhou, *et al.*, "Large scale interactive motion forecasting for autonomous driving: The waymo open motion dataset," in *Proceedings of the IEEE/CVF International Conference on Computer Vision*, 2021, pp. 9710–9719.